Materials Research Bulletin 97 (2018) 222–231

Contents lists available at ScienceDirect

Materials Research Bulletin

journal homepage: www.elsevier.com/locate/matresbu

Fabrication and characterization of tin-modified TNT via different tin compounds treatment

Cheng-Yen Tsai, Chen-Wuing Liu*, Li-Chi Lai, Yi-Wen Lin

Department of Bioenvironmental Systems Engineering, National Taiwan University, No. 1, Section 4, Roosevelt Road, Taipei 106, Taiwan

ARTICLE INFO

Keywords:
Photocatalysis
Electron-hole recombination
Oriented attachment mechanism
Calcination-free
Hydrothermal method

ABSTRACT

This paper presents the fabrication, characterization, and testing of the photocatalytic potential of a non-modified titania nanotube (TNT) and Sn-modified TNT synthesized through a facile one-step hydrothermal method. Two tin compounds ($SnCl_2$ and SnO_2) and aqueous solutions (HCl and $SnCl_2$) were utilized as precursors and acid washing solutions, respectively. Because the Sn-modified TNT was free of calcination, the resulting sample possessed a high Brunauer-Emmett-Teller surface area. In addition, the Sn-modified TNT exhibited higher electron-hole separation efficiency. The photocatalytic reaction rate for the sample with methylene blue and malachite green dye decomposition was governed on the basis of their pre-adsorption abilities. The Sn-modified TNT had more Cl species than the non-modified TNT, resulting in higher pre-adsorption abilities for the methylene blue dye. Even though the Cl species on SnO_2-TNT sample surface were removed, a higher electron-hole separation efficiency and anatase-rutile mixed phase can promote the photocatalyst activity of SnO_2-TNT. On the other hand, the Cl species on the surface of SnO_2-TNT-HCl washing sample appeared to act as one of the adsorption sites and enhance gaseous elemental mercury removal.

1. Introduction

Titania nanotubes (TNT) have high specific surface area, nanotubular structure with layered walls, and photocatalytic activity that can decompose various contaminants in aqueous phases. Since Kasuga et al. [1] first reported the alkaline hydrothermal synthesis TNT, subsequent researchers have employed this method to fabricate different non-modified TNT or TNT composites. The advantages of the hydrothermal method include low cost, easy operation, and low synthesis temperatures. To enhance the photocatalytic reaction rate, the TNT crystals may be required to undergo additional calcination because of the relatively low processing temperature of the hydrothermal method [2–5]. Nevertheless, the phase transition of TNT through calcination generally results in the over-conversion of tubular structures into particles. The calcination treatment is not only multi-step fabrication process but also decrease in the surface area of the TNT. This renders unnecessary the synthesis of a nanotubular structure by using crude TiO_2 nanoparticles. Thus, fabricating the non-modified TNT or TNT composites with a calcination-free or eschewing multi-step production process is profitable.

By contrast, TNT synthesized through metal-oxide modification, for example SnO_2 [6–11], CuO [12–14], and Al_2O_3 [15], can enhance electron-hole separation efficiency, which improves the photocatalytic activity of TNT. Several reports indicated that there is a suppressing of the recombination process by coupling two different semiconductors with dissimilar Fermi levels, i.e. the introduction of SnO_2 to the TiO_2 produces a more efficient separation of the photogenerated pairs [16–19]. SnO_2 and TiO_2 possess a similar rutile-type tetragonal structure, electronic properties, and ionic radii; therefore, the use of Sn-modified TNT has attracted increasing research attention [20–22].

Tsai et al. fabricated Sn^{2+}-incorporated TNT by washing sodium titanate with a $SnCl_2$ solution. Oxidation of the Sn^{2+}-incorporated titanate nanotubes resulted in the oxidation of Sn^{2+} to Sn^{4+}, thereby, widening the band gap. Moreover, they reported that the byproduct of SnO_2 crumbs was formed through the following reactions after $SnCl_2$ washing, which was attached to the nanotubes [23].

$$Sn^{2+} + 2OH^- \rightarrow SnO_2 + H_2 \tag{R1}$$

$$Sn^{2+} + 2H_2O \rightarrow SnO_2 + H_2 + 2H^+ \tag{R2}$$

Zhao et al. manufactured SnO_2/TNT composites and calcined them at 300 °C. First, they used P-25 and 10 M NaOH to synthesize the TNT powder. Then, SnO_2/TNT composites were fabricated by mixing the TNT powder and $SnCl_2$ in a 0.1 M HCl solution. These hetero-nanostructured photocatalysts with increased specific surface area could offer more active sites when in contact with contaminants, resulting in

---

* Corresponding author.
E-mail address: cwliu@ntu.edu.tw (C.-W. Liu).

http://dx.doi.org/10.1016/j.materresbull.2017.09.003
Received 23 April 2017; Received in revised form 8 August 2017; Accepted 2 September 2017
Available online 04 September 2017
0025-5408/ © 2017 Elsevier Ltd. All rights reserved.

improved photocatalytic activity [24]. Mourão et al. mixed commercial TiO_2 and $SnCl_2 \cdot 2H_2O$ in an aqueous KOH solution, generating TiO_2/SnO_2 heterostructures [25].

Although anterior methods can be employed for synthesizing SnO_2-TNT composites, multistep procedures, including TiO_2 nanotube fabrication, mixing of TNT with $SnCl_2 \cdot 2H_2O$ aqueous, and subsequent calcination, are required. In our previous study, a simple, cost-effective, and environmentally friendly synthetic strategy was developed for the preparation of SnO_2-TNT composites, wherein the resulting sample was free of calcination [26]. In the present study, we followed our prior synthetic method using two tin compounds ($SnCl_2$ and SnO_2) and acid solutions (HCl and $SnCl_2$) to synthesize non-modified and Sn-modified TNT composites. The obtained samples were analyzed through N_2 adsorption isotherms, X-ray diffraction (XRD), transmission electron microscopy (TEM), photoluminescence spectroscopy (PL), zeta potential and X-ray photoelectron spectroscopy (XPS). The photodegradation and adsorption efficiencies of the samples were examined for the degradation of methylene blue (MB) and malachite green (MG) dye solutions under ultraviolet (UV) irradiation. Furthermore, the photocatalytic activity of TNT for aqueous-phase dye decomposition depends on their adsorption abilities. Cui et al. indicated that inorganic counterions, especially halide ions, can form ion pairs with MB [27]. In order to investigate dye adsorption efficiency influenced by the Cl content on the sample surface, the adsorption efficiencies of the non-modified TNT, Sn-modified TNT and Cl^- removed samples were determined to better explain the synthesis characteristics of the TNT surface. On the other hand, the photocatalytic performance of three TNT samples with HCl treatment was comprehended based on the low-concentration (ppb_v level) gaseous elemental mercury (Hg^0) removal experiment.

2. Materials and method

2.1. Preparation of non-modified TNT and Sn-modified TNT nanocomposite

This study synthesized the Sn-modified TNT via a hydrothermal method from TiO_2 nanoparticles (Degussa P-25 TiO_2), $SnCl_2 \cdot 2H_2O$ (Alfa Aesar 98%) and cassiterite SnO_2 (Alfa Aesar 99.9%). The hydrothermal process was similar to that described by a previous report [28]. TNT was synthesized by 5 g of P-25 TiO_2 that was added into a 200 mL of 10 M NaOH aqueous solution in a Teflon-lined autoclave at 130 °C for 24 h. Subsequently, the product was washed with 0.5 N HCl (or $SnCl_2$ solution) and distilled water until the pH value of the washed solution reached around 3.5. After that, the samples were dried at 100 °C for 24 h. The formed TiO_2 nanotube was designated as TNT-HCl washing (or TNT-$SnCl_2$ washing). Sn-modified TNTs were fabricated by the similar process to synthesize the Sn-modified TNTs with 5 wt.% $SnCl_2$ (or SnO_2), the products were designated as $SnCl_2$-TNT-HCl and SnO_2-TNT-HCl washing sample. Moreover, in order to compare with calcination-free TNT, some TNT-HCl washing samples were calcined from 300 to 600 °C.

2.2. Characterization of TNT and Sn-modified TNT nanocomposite

Brunauer-Emmett-Teller (BET) specific surface area was determined by using a Micromeritics ASAP 2020 based on the N_2 adsorption isotherm obtained at 77 K. Powder X-ray diffraction (XRD; Bruker, D2 Phaser) with Cu Kα radiation ($\lambda = 1.5405$ Å) was used for crystal structure identification. The crystalline phases were identified with JCPDS database. The morphology of as-prepared samples was examined using a transmission electron microscope (TEM; Hitachi H-7100). Photoluminescence spectroscopy (PL) was carried out using a fluorescence spectrometer (Horiba Fluoro Max-4) under excitation with 330 nm irradiation. The zeta potential of sample was determined with Malvern Zetasizer 3000HS. The composition and Ti 2p, O 1s, and Sn 3d bonding patterns were analyzed by an X-ray photoelectron spectroscope (XPS; VG Scientific ESCALAB 250). The obtained XPS spectra were deconvoluted with the XPSPEAK software. All binding energies (BE) were referred to C 1 s peak at 288.5 eV. The Cl content of the sample was analyzed by using an X-ray energy dispersive spectrometer (EDS, JEOL JSM-7000F).

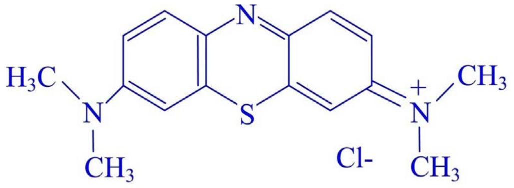

Methylene Blue

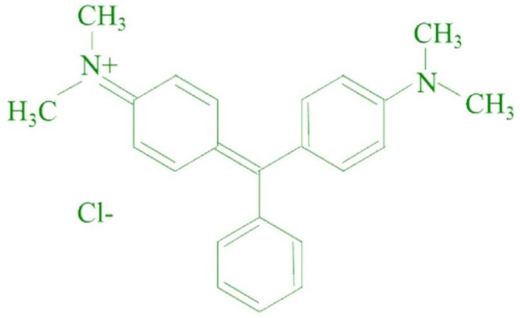

Malachite Green

Fig. 1. The chemical structure of dyes methylene blue and malachite green. (For interpretation of the references to colour in this figure legend, the reader is referred to the web version of this article.)

2.3. Dye photocatalytic reaction rate evaluation

The photocatalytic activity of the sample was carried out by photodegradation of methylene blue (MB) and malachite green (MG). The chemical structures of MB and MG dye are illustrated in Fig. 1. The tests were performed in a 100 mL photochemical reactor containing 10 mg of sample and 15 ppm of MB/or MG aqueous solution. Two UV lamps (80 W, Raceahead Co., Taiwan) that possessed a major sharp peak at 254 nm (Rainbow Light RLS-1000, Taiwan) was employed and placed at 20 cm away from the reactor. The UV intensity (3.0 ± 0.1 mW/cm^2) was determined by Sentry UVC-ST512 equipment. A quartz flake was located on the reactor to evade any contact between the atmosphere and the solution. The conclusion of the decomposition efficiency was calculated by the following equation:

$$\textit{Decolorization efficiency}\ (\%) = \frac{C_0 - C_i}{C_0} \times 100\% \tag{1}$$

where C_0 is the initial concentration of the dye and C_i is the dye final concentration after illumination by UV-light for 60 min. Moreover, the MB/or MG adsorption estimation used 10 mg of sample and 15 ppm MB/or MG aqueous solution under dark condition for 60 min. All photodegradation and adsorption tests were duplicated. After photodegradation or adsorption experiment, the solution was used a centrifuge (8000 rpm for 20 min) to separate MB solution and TNT sample. The solution MB/or MG concentration was measured by a UV–vis spectrophotometer (Thermo Genesys-20), which λ was set at 670 nm (for MB) and 621 nm (for MG). All photodegradation and adsorption of dyes experiments were carried out at room temperature.

Download English Version:

https://daneshyari.com/en/article/5441733

Download Persian Version:

https://daneshyari.com/article/5441733

Daneshyari.com